Renewable Energy 227 (2024) 120479

Contents lists available at ScienceDirect

Renewable Energy

journal homepage: www.elsevier.com/locate/renene

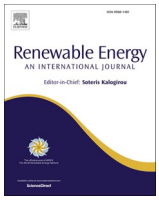

Agglomeration behaviour of various biomass fuels under different air staging conditions in fluidised bed technology for renewable energy applications

Farooq Sher [a,*], Narcisa Smječanin [b,c], Muhammad Kashif Khan [d], Imran Shabbir [e], Salman Ali [c], Mohammad Rafe Hatshan [f], Irfan Ul Hai [a,c]

[a] Department of Engineering, School of Science and Technology, Nottingham Trent University, Nottingham, NG11 8NS, United Kingdom
[b] Department of Chemistry, Faculty of Science, University of Sarajevo, Sarajevo, 71000, Bosnia and Herzegovina
[c] International Society of Engineering Science and Technology, Nottingham, United Kingdom
[d] School of Chemical Engineering, Sungkyunkwan University, Suwon, 16419, South Korea
[e] Energy Department, Tata Steel, Port Talbot Works, Port Talbot, SA13 2NG, United Kingdom
[f] Department of Chemistry, College of Science, King Saud University, P.O. Box 2455, Riyadh, 11451, Saudi Arabia

ARTICLE INFO

Keywords:
Renewable energy
Biomass fuels
Fluidised bed combustion (FBC)
Air-staging
Clean environment
Emissions
Bed agglomeration and net zero

ABSTRACT

The most common technology for thermochemical conversion of solid fuel through the process of gasification, such as coal, varieties of residues from biomass and agriculture are the bubbling fluidised bed or fluidised bed systems. However, there are some disadvantages within these systems including the formation of eutectic mixtures, increased process of melting and bed agglomeration. Hence, the current study aimed to evaluate the agglomeration behaviour of various biomass fuels. Characteristics of five biomass fuels (miscanthus, peanut, straw, domestic wood and industrial wood) in a bubbling fluidised bed (BFB) combustor were studied by SEM-EDX, XRD and XRF analysis of bed materials and ash samples. The influence of bed temperatures on the fuel ash composition and bed particles was evaluated, as well as fuel ash components, their interaction with the particles from the bed sand and morphology of the bed material. The combustion efficiency ranged from 95.5 to 99.5% with the highest value obtained for miscanthus under SA conditions. The peanut and straw had the highest K content, whereas the industrial wood ash contained the highest Ca content compared to other biomasses. The XRF results showed that most of the potassium (K) from the wheat straw biomass was converted to K_2O with 19%. No bed agglomeration was noticed without staging-air (WSA) and with staging-air (SA) combustion conditions, even with temperatures up to 850 °C during the testing period. Overall obtained results demonstrated that agglomeration is unlikely expected to be a major problem during fluidised bed combustion of tested biomass fuels.

1. Introduction

Biomass appears to be an attractive energy option that could be used to generate heat, electricity or different forms of power [1]. Biomass's global energy potential is widely recognised because it is the fourth largest source after oil, coal and natural gas [2]. Recently, biomass has drawn worldwide attention as an energy source because it is a renewable source, highly productive, carbon neutral and easy to store and as well to transport [3,4]. Regardless of broader applications of fluidised beds (FBs) for the conversation of solid fuels into energy, the technology is still facing some technical challenges; among others, agglomeration is one of the major operational issues during the combustion of solid fuels including biomass [5,6]. Agglomeration and sintering issues are more commonly found in low-ranked coals and biomass applications [7]. The ash produced during combustion process is considered one of the major influential constituents for agglomeration and sintering formation even in the absence of the other present factors in the FBs [8]. The characteristic of ash obtained from biomass differs from coals, due to their many plant varieties and the growth conditions. Biomass ash is usually dominated by calcium, potassium, silicon and a small amount of aluminium [9]. Therefore, it is a well-established fact that the agglomeration and sintering problems related to ash usually develop between

* Corresponding author. Department of Engineering, School of Science and Technology, Nottingham Trent University, Nottingham, NG11 8NS, United Kingdom.
E-mail address: Farooq.Sher@ntu.ac.uk (F. Sher).

https://doi.org/10.1016/j.renene.2024.120479
Received 23 August 2023; Received in revised form 23 February 2024; Accepted 8 April 2024
Available online 9 April 2024
0960-1481/© 2024 The Authors. Published by Elsevier Ltd. This is an open access article under the CC BY license (http://creativecommons.org/licenses/by/4.0/).

the ash particles and bed materials during the combustion process in the FBs [7]. Moreover, the ability for agglomeration and sintering formation also depends on many other factors such as fuel type, bed material used and localised temperatures during combustion [10,11].

Many researchers identified that agglomeration [12] and sintering are also associated with the composition of biomass, mainly alkali and alkaline earth metals (including their oxides) as these inorganic metals influence the type of alkaline silicates formed during the process of combustion [13]. However, it is vital to identify the elements (alkali or/and alkaline earth metals) causing the agglomeration in biomass fuels. For detailed investigations of the agglomeration and sintering, the surface morphology study of the formed agglomerates is necessary. The surface morphology investigations reveal [14] that agglomeration and sintering are heavily influenced by different combustion stages and temperatures (from the burning of char particles) during the combustion of different fuels and there are only a few studies about it [11]. In the study of Chi et al. [14] surface morphology analysis was used to evaluate the mechanisms of anti-agglomeration when adding additives under different conditions of combustion.

Although agglomeration and sintering have been widely studied considering the combustion of coal and co-combustion of coal with the different biomasses. However, much less attention is being paid to the agglomeration problems resulting from biomass combustion and gasification in FBs systems. In addition, the mechanisms responsible for agglomeration and sintering during biomass combustion in FBs suggested by other researchers need to be further studied in detail to know the applicability of these mechanisms. In the study of Yao et al. [15] was found that the addition of K_2CO_3 promotes agglomeration when added to the mixture of soybean straw and coal. Furthermore, a study conducted by Wagner et al. [16] evaluated the mechanism of K-feldspar layer formation in BFBC of biomass that was rich and lean in phosphorus. It was found that the addition of phosphorus-rich biomass residue to the wheat straw as fuel in FBs system is reducing the tendency for bed agglomeration by increasing the melting temperature of the produced ash [16].

Accordingly, in the present study, the main fundamental aspects related to the agglomeration and sintering phenomena were investigated for biomass fuels combusted under air in a bubbling fluidised bed combustor (BFBC). The detailed findings regarding characterisation of bed materials and ash samples collected from all experiments during air and oxy-fuel combustion are reported and discussed. Five different types of biomasses including; miscanthus, peanut, straw, domestic and industrial wood were used as fuels. The biomass fuels and bed material before and after combustion in bubbling fluidised bed combustor (BFBC) were characterized by scanning electron microscope (SEM) and energy dispersive X-ray (EDX), X-ray diffraction (XRD) and X-ray fluorescence (XRF) analysis. The discussion also covers different types of observations that include surface morphology, weight and colour changes of the bed material particles for different biomass fuel types tested in BFBC system. Obtained combustion efficiency, the effect of temperature on different experimental conditions as well as obtained gas products have been discussed. Results of the current study will give valuable insight into agglomeration problems during biomass combustion and could serve for further studies and prediction of biomass mechanism development due to the combustion in BFBC.

2. Experimental setup and analysis methods

Five biomass fuels were tested in BFB combustor; domestic and industrial wood as woody biomass and miscanthus, straw and peanut as non-woody biomass. All fuels were organised from the UK. They were in pellet form with a size range from 10 to 20 mm. The ultimate, proximate analysis along with the heating values of these fuels is given in Table 1. A schematic diagram of the BFB combustor is represented in Fig. 1. The rig was composed of a main reactor a feeding system for biomass, an air blower fan, downstream rig consisting of a cyclone, gas cooling, cleaning and analysis system. The feeding unit involved a hopper, ager and geared motor, the speed of the motor was controlled by an inverter. Biomass was loaded from the feeder hopper into the system of the reactor by using a horizontal screw conveyor. Adjustment of the screw feeder was established through the calibration for all types of biomasses used to account for alterations in particle size and content of moisture in a given batch utilized system. The main combustor reactor dimensions were 800 mm (height) and 102 mm (internal diameter) for the bed zone. A sintered stainless steel plate was used as a distribution plate with a thickness of 12 mm and pore size of 0.002 mm. A bed of Garside silica sand 14/25 with a sauter mean diameter (d_{32}) of 0.78 mm was fluidised using air that enters from the reactor base into the plenum with an internal diameter of 102.2 cm. Biomass fuel was introduced into the sand bed that is combusted using the fluidising (primary) air. A very small fraction of air (feeder air) was also introduced into the feeder to stop any kind of backfire. The hot gases produced after combustion pass through a high-efficiency cyclone that removes sand and ash particles from the gaseous stream.

The ash and particulate fine matter were collected from the cyclone after every run from the routinely emptied ash can. To maintain a satisfactory BFB combustion operation, the bed was opened after two to three runs and bed material was removed to observe any type of agglomeration during the combustion of a specific type of biomass fuel. The combustor was heated with two ceramic fibre heaters 2100 W installed around the body of the main reactor. Overall combustor including the main reactor, the riser and the cyclone is protected with ~50 mm of high-temperature fibre isolation to preserve temperature in the rig. The external reactor wall temperature was controlled by digital controllers by the installed thermocouple. The primary air was supplied from the bottom of the reactor through a blower fan using a 5 cm stainless steel flexible hose. An in-house air compressor was used to supply the feeder with the air. For the primary airline, a flexible electric heating tape was installed on the line that ensures heat to increase the temperature to ~450 °C of the inlet air. A heat extraction water cooling

Table 1
Ultimate and proximate analysis with calorific values of utilized biomass fuels [17].

Biomass fuels	Ultimate analysis[a]					Proximate analysis[c]				
	C (%)	H (%)	N (%)	O[b] (%)	S (%)	M (%)	VM (%)	FC (%)	Ash (%)	HHV[d] (MJ/kg)
Domestic wood	47.18	6.84	0.17	45.65	0.17	3.94	85.11	14.19	0.70	19.81
Industrial wood	47.57	6.95	0.26	45.02	0.21	5.34	85.00	13.72	1.28	20.13
Miscanthus	45.87	6.74	0.38	46.82	0.19	3.34	82.85	15.37	1.80	19.10
Straw	43.80	6.78	0.55	48.29	0.58	5.22	76.31	17.54	6.23	18.21
Peanut	46.97	6.79	1.34	44.38	0.51	5.96	74.06	22.40	3.55	19.77

M: moisture, VM: volatile matter, FC: fixed carbon, LHV: lower heating value, HHV: higher heating value.
[a] On dry basis except as denoted in the table.
[b] Calculated by difference.
[c] On dry basis except moisture which is as received basis.
[d] Calculated based on [47].

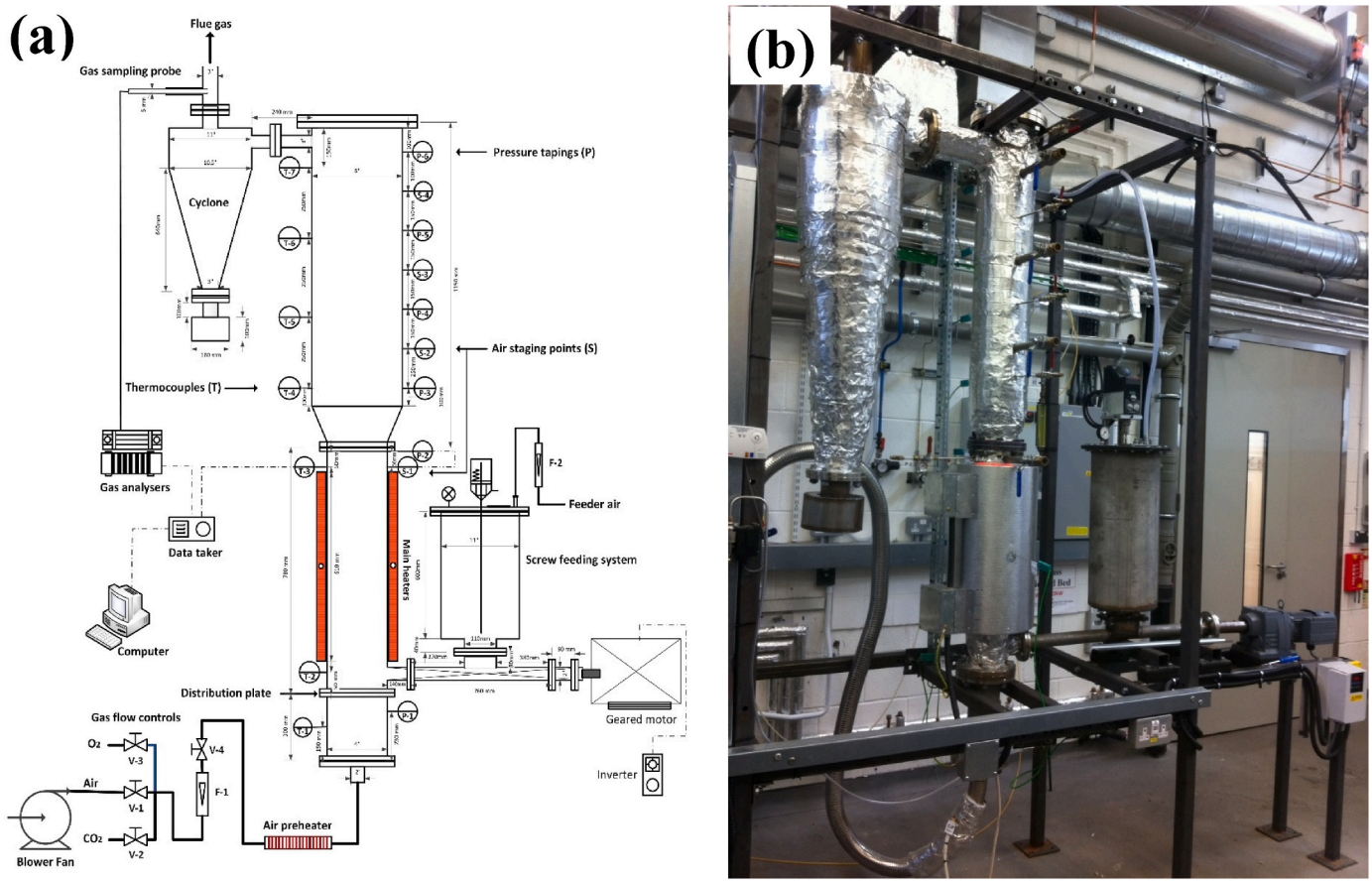

Fig. 1. Experimental setup of bubbling fluidised bed combustor (BFBC); (a) Schematic representation [17] and (b) Actual setup, rig installed in the lab.

probe is introduced from the top of the reactor to control the excessive temperatures inside the reactor during operation. Another water-cooling probe is installed at the exit of the cyclone for gas sampling analysis. Water for cooling was provided to the rig from the normal water supply in the lab. Following the flue gas cleaning section of the rig, the flue gas was cooled in two dreschel bottles connected in series. The dreschel bottles are kept in an ice bath to cool the gas close to ambient conditions. The condensable compounds and tars contained within the gas stream are retained in the filters connected after the bottles during the process of cooling. After the cooling process, the gas stream was sent to gas analysers where it was analysed and later on, vented to the atmosphere through the exhaust.

2.1. Procedure and operating conditions

Garside silica sand size $\leq$1 mm added with a 2655 kg/m^3 up density to a height of 25 cm (3.2 kg) used as the insert bed material that was topped up from the top flange of the reactor. The operation temperature was in the range of 750–850 °C, but the rig could operate at up to ~1000 °C. The rig worked at atmospheric pressure and was used for biomass combustion either using air and/or gas mixtures like oxy-fuel (O_2/CO_2). Biomass could be loaded into the reactor system up to ~6 kg/h at a feed rate. The minimum velocity of air inside the reactor ranged from 2 to 5 m/s. The flow rate of cooling water varied from 1 to 1.4 L/min, depending on selected temperatures within the reactor. At the beginning of each experiment, a variety of operations are performed to heat up the rig. The inlet primary air flow rate to the reactor is started at 300 L/min and feeder air at 50 L/min at STP. The main ceramic heaters then worked with a selected point of 850 °C at the outside wall of the reactor system to preheat the reactor before the test. Then flexible air preheater is set at 450 °C to start heating the air entering the reactor. Once the sand bed was heated to +500 °C, the biomass was loaded at the selected flow rate for combustion starting. When the proper combustion process starts the main and preheater are switched off. A water-cooling heat extraction probe was inserted from the top of the reactor to control temperature inside without leading to agglomeration and/or defluidisation.

The key parameters trends (Differential pressures, bed temperature profiles, freeboard temperature profiles, and flue gas composition) were continuously monitored. The data of all these parameters were recorded every 10 s through a data taker in the computer. A sudden alteration in the drop of pressure over the bed, followed by a great increase in the temperature above the bed, implied loss of fluidization, called bed fluidization. In the case of defluidization during the experiment, all further testing was immediately stopped that meant the selected operating parameters were not convenient for an industrial application. The combustion experiments were run for up to 12 h per day due to extensive heat-up and cool-down times. At the end of every experiment conducted, the biomass feeder was stopped and bed was left to cool down to the temperature of ambient. The bed and cyclone were opened to remove materials then examined and analysed. The presence of agglomerates as big clumps of sand particles in bed material implicated that set-up operating requirements of experiment could sooner or later cause a problem, nevertheless whether problems are observed during the actual test.

The WSA tests (without air staging) were carried out with continuous biomass feeding in BFBC and the results were obtained under steady-state conditions. The combustor was left to carry on with the operation at these terms and stabilise to between 750 and 850 °C of bed temperatures. To evaluate the influence of the excess air on the flue gas emissions and combustion efficiency, different excess air ratios including; 15, 30 and 45% were studied by changing the biomass fuel

feed rates and by keeping an overall rate of air flow constant at 350 L/min. The temperature along the freeboard and reactor varied with the variation of fuel feeding rate, due to the unchanged flow rate of the water and the position of the cooling probe. To assess the influence of the air staging, 50 L/min of a part of the overall rate of air flow was redirected to one of the air staging injection pipes and the overall rate of air flow was set up at 350 L/min constant value. At the heights of 70 cm (named SA1) and 110 cm (named SA2) the secondary air was injected from the plate of distribution to assess the way the SA injection location influenced the composition of the gas. On the other side, tests at WAS conditions were also complete with all the selected biomass fuels. Three or four runs at least were carried on with every selected biomass for different tested terms (WSA, SA1 and SA2), to support the achieved results. A matrix showing all the tests performed under different conditions is shown in Table 2. In addition, the performance of BFBC for all types of utilized biomass fuels at different operating conditions was measured by calculating combustion efficiency reported in the study of Llorente and Cuadrado [18] using **Eq. (1)**. Where CO_2 and CO quantities represent volumetric basis measured through the gas analysers during combustion in the flue gas.

$$\eta = \frac{\%CO_2}{\%CO_2 + \%CO} \times 100\% \quad (1)$$

2.2. Bed material and cyclone ash sampling

After completing the combustion experiments with each type of biomass fuel under one set of conditions (air, air staging or oxy-fuel) the bed was opened for visual inspection and sample collections. The BFBC system was cooled down to the temperature of a room and the fluidising air stainless steel pipe associated with the plenum chamber was separated. The previously mentioned was accompanied by the separation of frame supporting bars of fluidised bed section running through bottom of the plenum chamber flange. A rectangular plastic sheet of size 1500×1000 mm was laid on the floor to collect the bad material sand. After removing metal parts that are fixing the chamber for the plenum and plate for distribution to the zone of fluidization were separated and the sand was left to flow out and pour onto the sheet of plastic. The collected bed material was visibly evaluated for signs of any type of agglomeration or sintering and weighed.

A portion of the bed material was stored and packed into labelled sample bags for further processing. The sampled portion of the bed material 100–200 g was grounded into a powered form of size <50 μm using a mill and stored in plastic bags for further analysis using SEM-EDX, XRD and XRF. The above procedure was repeated for the collection of second and tired samples to prepare for the experiments with a new batch 3.2 kg of fresh Garside 14/25 sand (size ≤1 mm) added to the reactor as the new bed material. The distribution of particle size for used sand with a size ≤1 mm is given in Table 3. During the combustion of biomass in the BFBC system, the solids including ash, char and/or particles of bed material entrained in the up-through flue gas from the reactor and ending up in the cyclone are collected by the cyclone reject container and termed as cyclone reject. After each day's run, the cyclone container was opened and all collected material was weighed and stored in labelled plastic sample bags. A portion of cyclone ash samples was ground following the same method as previously mentioned, SEM-EDX, XRD and XRF.

2.3. Characterisation of bed material

Two types of techniques for SEM sample preparation were used during this analysis. With the first technique, a small amount of material was bound on a carbon sticky table and was then analysed under SEM to investigate the images. With the second technique, the material was ground into a fine powder (size <50 μm) using the method described in section 2.2 then first a pellet with a diameter of 5 mm and a thickness of 2 mm was prepared from the powder using a hydraulic press and finally, the pellet was analysed under the SEM to get detailed information about the chemical compounds present in the material. The unground sample material provides quality SEM images. The SEM analysis was done by the backscattered electron (BSE) type detector, at 20 kV working under a mode of low vacuum for carbon tabs and high vacuum for ground pellets. The interactive oxides mode method was used for the quantification of materials under SEM-EDX in the present research. The spectra' working distance was 14 mm and the micrographs were recorded at various magnifications of 50, 100, 150 and 300 times. During SEM-EDX analysis the spectra working distance was fixed at 13 mm and the high

Table 3
Sand particle size distribution for size <1 mm.

Particle Size (mm)	Weight (gm)	Grading (%)	Radius	Vp (kg/m^3)	Ap (m^2)	xi/dpi
0.85	1072.60	38.69	0.43	0.32	2.27	1261.88
0.60	1646.82	59.40	0.36	0.20	1.65	2744.70
0.30	49.92	1.80	0.23	0.05	0.64	166.40
0.21	2.20	0.08	0.13	0.01	0.21	10.38
0.15	0.67	0.02	0.09	0.00	0.10	4.46
0.00	0.23	0.01	0.04	0.00	0.02	0.00

Table 2
Experimental matrix for the tests performed without air staging and with air staging combustion.

Batch No.	Biomass fuel type	Combustion environment	Fuel feed rate (kg/h)	Excess air level (%)	Temperature range (°C)	Cooling water flow rate (L/min)	Number of runs	Total run time (h)
1	Domestic wood	WAS	3–5	10–50	750–850	1.2	4	8–12
	Industrial wood	WAS	3–5	10–50	750–850	1.2	4	8–12
	Miscanthus	WAS	3–5	10–50	750–850	1.0	4	8–12
	Peanut shell	WAS	3–5	10–50	750–850	1.0	4	8–12
	Wheat straw	WAS	3–5	10–50	750–850	1.0	4	8–12
2	Domestic wood	AS 1	3–5	10–50	750–850	1.2	4	8–12
	Industrial wood	AS 1	3–5	10–50	750–850	1.2	4	8–12
	Miscanthus	AS 1	3–5	10–50	750–850	1.0	4	8–12
	Peanut shell	AS 1	3–5	10–50	750–850	1.0	4	8–12
	Wheat straw	AS 1	3–5	10–50	750–850	1.0	4	8–12
3	Domestic wood	AS 2	3–5	10–50	750–850	1.2	4	8–12
	Industrial wood	AS 2	3–5	10–50	750–850	1.2	4	8–12
	Miscanthus	AS 2	3–5	10–50	750–850	1.0	4	8–12
	Peanut shell	AS 2	3–5	10–50	750–850	1.0	4	8–12
	Wheat straw	AS 2	3–5	10–50	750–850	1.0	4	8–12

voltage was set at 20 kV. A range of magnifications (500, 200, 100 and 50 ×) with an image working distance of 14 mm were used to get clear and magnified images of the samples with the selection of magnification being made according to the area of interest. For EDX spot analysis, the interactive oxides method was applied to detect the exact composition of elements on a specific point of the agglomerate [19].

In the present research, the powder X-ray diffractometer D500 system was used. The powdered sample for X-ray diffractometer analysis was prepared using the same method as described in section 2.2. The system was equipped with a sample holder for 9 samples that could perform even overnight scans. The powdered diffractometer was operated with a parallel beam and very low intensity to estimate the phases with more than 1% presence in the material. The method used in the powdered diffractometer was CuKα radiation and scanned from 10 to 80 °2 θ angles with 0.05 °2. The θ angle step size and 6 s time per step. As for results evaluation and analysis, TOPAS V5 software was used. The crystallinity (amount of crystalline phase vs. total) was estimated by presuming the same elemental composition of the amorphous phase(s) as the crystalline. The TOPAS V5 is a Rietveld refinement [20] software and uses the principles of Hill and Howard [21] for quantities' computation.

The XRF analysis of characterisation was performed using powdered samples in the form of 10 mm and 5 mm size diameter length pressed pellets. These pellets were pressed and then prepared by milling the material into powder size <50 μm using a Ring and Puck mill. The obtained results were analysed by the Spectra Plus software version 2.0 and Quant-express software. For XRD, the powder X-ray diffractometer with a parallel beam and very low intensity was used. The CuKα radiation was applied and scanned from 10 to 80 °2θ with 0.05 °2θ step size and 6 s per step. As for evaluation, TOPAS V5 software was used and the crystallinity (number of crystalline phases vs. total) is estimated presuming the same elemental composition of the amorphous phase(s) as the crystalline.

3. Results and discussion

Five selected types of biomass fuels including; industrial wood, domestic wood, miscanthus, wheat straw and peanut shell pellets were tested in a 20 kW_{th} bubbling fluidised bed combustor (BFBC). As mentioned previously Garside 14/25 sand was utilized as a bed material during all combustion experiments. The testing was not a continuous process with each test lasting for 8–12 h of operation. For repeatability and authenticity of the produced results, each biomass fuel was tested for 3–5 repeated runs with a total of 30–36 h of operation. The average temperatures in the BFBC during combustion under air were between 750 and 850 °C. The agglomeration or sintering could cause fluidization that leads to unscheduled plant shutdowns and extra costs for maintenance. In accordance with the research of Sevonius et al. [22] defluidisation could be indicated by a sudden decrease in the pressure drop across the bed. The temperatures are another indicator during fluidization. Just before fluidization, the bed temperatures rise rapidly due to poor mixing of fuel in the bed zone [14]. All the temperature and pressure parameters were consistently monitored during the testing, but there was no defluidisation observed during any biomass fuel combustion in the BFBC.

3.1. Combustion efficiency analysis

The results from the comparison of combustion efficiencies for different biomass fuels at conditions (WSA) without air staging, with air staging level one (SA1) and air staging level two (SA2) experiments based on the emissions without considering unburnt carbon in the fly ash are given in Fig. 2. The combustion efficiency ranged between 95.5 and 99.5%. The combustion efficiency for all tested biomass fuels has improved under air staging conditions. The highest combustion efficiency 99.2 and 99.1% was noticed for miscanthus under air staging SA1

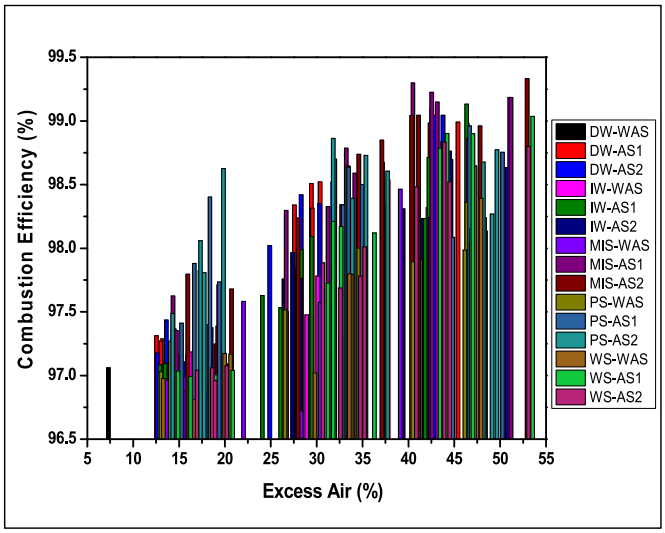

Fig. 2. Comparison of combustion without considering carbon in the fly ash for all types of biomass fuels under WSA, SA1 and SA2 conditions. The plotted results are averaged from several test runs.

and SA2 conditions respectively, followed by wood pellets with 99% under SA2 using 45% excess air. In general, the combustion efficiency was lower in the case without air staging combustion with less excess air. All biomass fuels were burned successfully under air staging with a marginal difference in their combustion efficiency. As the level of excess air decreased, there was not enough oxygen in the reactor to complete the combustion, hence combustion efficiency dropped. This was understandable since the total airflow to the combustor was limited. In addition, there was more fuel accumulated (fuel-rich conditions) in the bed region and an increase in bed zone residence time thus resulting in a shorter residence time in the freeboard, i.e. a reduced burnout time for the fuel char particles thus resulting in a diminished combustion efficiency.

In another way, under fuel-rich conditions there is a low oxygen concentration in the bed zone that hindered the combustion and resulted in low efficiency. The drop in combustion efficiency was only marginal for the high volatile content fuels like industrial wood and miscanthus. The maximum drop in efficiency of combustion was 3.7% for miscanthus among all tested fuels. The gas temperature is another factor affecting the combustion efficiency. The obtained results also illustrated that combustion efficiency was higher for all tested biomass fuels under air staging conditions that could be attributed to higher gas temperatures during air staging with secondary air injection from different points as shown in Fig. 3. The higher gas temperatures could accelerate the overall combustion process thus resulting in higher combustion efficiency providing other conditions remained the same or similar. Park et al. [23] investigated the combustion and fluidization behaviour of rice husk in a bubbling fluidised bed reactor, they found that the temperature profiles in the reactor had a strong effect on combustion efficiency, thus the combustion efficiency increased with the temperature. The higher combustion efficiency in terms of emissions reduction was noticed when the staging air was injected from the highest point SA2 in all types of biomass fuels except peanut shell pellets.

The maximum value of temperature was achieved without air staging parameters (WAS) at the spray area and/or at the endpoint of the freeboard. The noted peak of temperature in freeboard (between SA1 and SA2) above dense bed is assigned to great amount of matter. That is volatile in utilized fuels and to its break and firing mostly in the spray area and freeboard, contrary to firing coal which is low volatile and its combustion is noted within a dense bed [24]. The process of segregation of biomass particles at the surface of the bed during devolatilization has been also noted in other similar studies [25]. The segregation is linked to

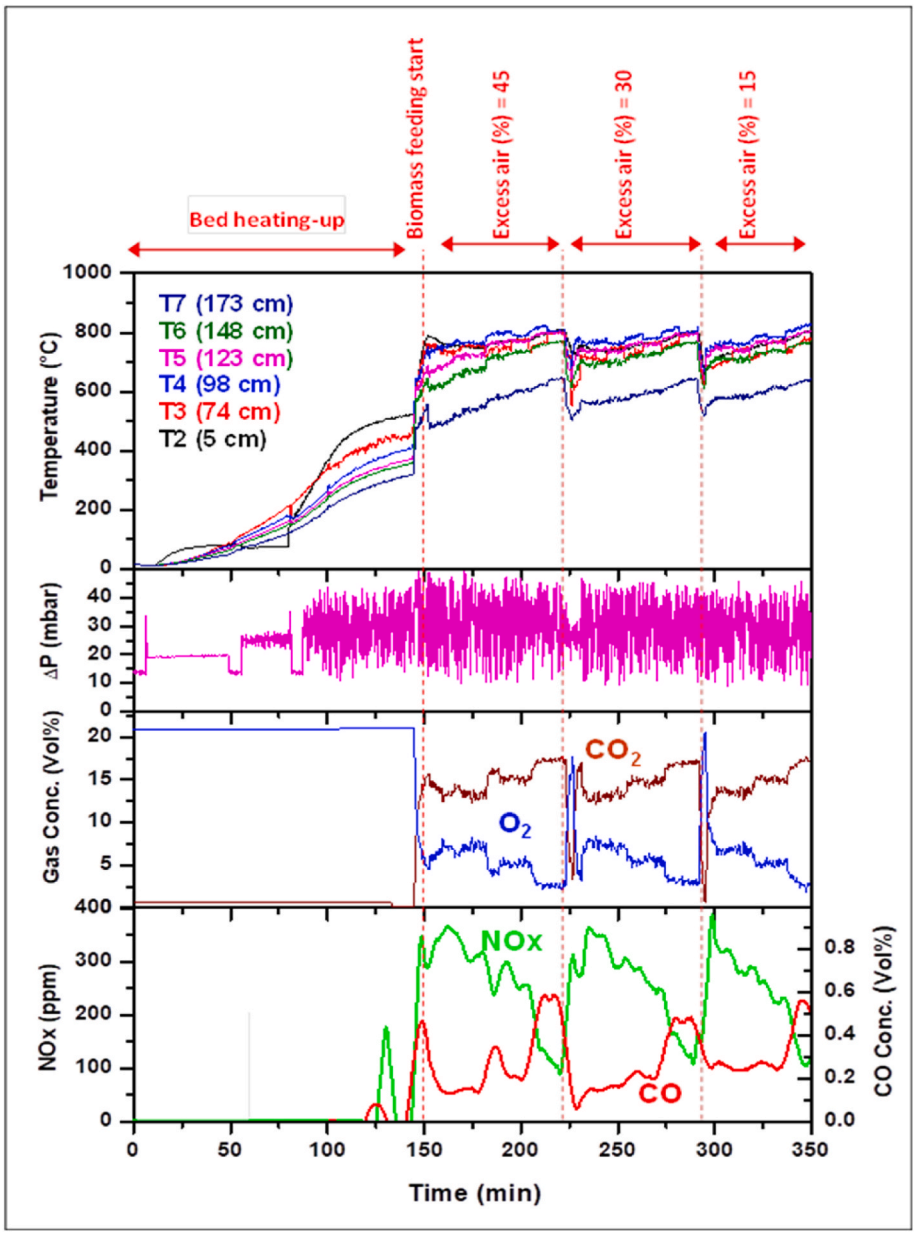

Fig. 3. Gas compositions at BFBC outlet for peanut shell combustion at WSA conditions with temperatures profile at various heights of the reactor and freeboard and pressure drop over dense bed.

the effect of lifting, bubbles that are volatilizing could bring on the particles of used biomass fuel. Temperature decreases above 1 m of freeboard after the peak of temperature is achieved. This is because when heat is extracted from upper section of the freeboard by water-cooling probe then released heat from the firing of any biomass that could not burn in freeboard area.

It is also noted from Fig. 3 that when SA1 and SA2 conditions were used with 10% level of air excess, temperature increases were very significant. This increase in temperature indicated that there is a notable quantity of gases that could not burn and volatile substances in the freeboard. As an outcome of combustion in sub-stoichiometric operating terms in the dense bed area and additional burnings of the unburned biomass in freeboard region after secondary air introduction. When SA was operating with an overall of 50% excess air, a decreased or same temperatures as in WSA conditions for all tested biomas fuels were noticed. The greater amount of air indicates higher combustion efficiency that could be accomplished in lower section of the reactor. There were almost no gasses or volatile substances that were not burned in freeboard area. After the input of secondary air temperature was decreased in many cases temporarily. Temperature decrease is because air before entering the combustor was not preheated that is why the temperature was lower than the temperature of the gas used for the combustion process. The previous case was more noticeable under SA1 conditions since a thermocouple was placed close to the mentioned point of injection.

Fig. 3 represents gas composition under WSA for peanut biomass. Similar trends were observed for other tested biomass fuels. Furthermore, this can be observed from Fig. 3, an increase in excess levels of air leads to increased NOx and decreased CO and CO_2 concentration at the reactor outlet. Increased NOx levels are due to the conversion of biomass/fuel-N to NOx in the atmosphere that is rich with O_2 in the combustor. Since it favours NOx formation and due to enhanced volatile matter and char combustion. Increased CO concentration is due to better combustion efficiency with excess air levels. Furthermore, feed rates with lower amounts of biomass caused less heat to be released and lower levels of CO_2 to be produced in the combustor. These observations are in

line with the results obtained in a study conducted by Gu et al. [26]. In addition, it was established that the composition of gas at BFBC outlet and temperature profiles along reactor were uniform under all experimental conditions and for all tested fuels.

3.2. Visual observations

At the end of each set of experiments with a specific biomass fuel, the bed of sand was opened for observations and samples were collected. Then the bed material was replaced with fresh sand for the next fuel testing. The bed materials collected after the combustion tests of all biomass fuels are shown in Fig. 4. From visual observations, it was discovered there were big black particles bonded together in the bed material during wheat straw pellets combustion, as shown in Fig. 4(e). It was also noticed that after each set of combustion tests, the bed materials changed into different colours depending on the biomass fuel used; from yellowish brown (original colour) to brownish black (domestic and industrial wood), grey (miscanthus), greyish black (wheat straw) and dark brown (peanut shell) colours. The change in the shape of the sand was also noticed in some cases after the combustion tests. The observed change in the colour of the sand was probably partly related to the thermal decomposition or oxidation of Fe_2O_3 that is present in Garside 14/25 sand material. Moreover, as found in the study of Kwong et al. [27] the change in the colour of the sand during combustion was found to be dependent on the temperatures and type of biomass fuel combusted with sand. The cyclone container was also emptied after each test run and the cyclone ash samples were collected for further analysis. These bed materials and cyclone ash samples were characterized to establish the mechanism of agglomeration and sintering tendencies during the combustion of different biomass fuels in BFBC.

3.3. Agglomeration during air combustion

A degree of agglomeration was found in the wheat straw pellet bed material as the sand particles were found to be bound with each other. The average size of the agglomerates was in the range of 2–4 mm after three testing runs, approximately 30–36 h of combustion time. The agglomerates were almost round shaped in black colour; it was difficult to distinguish between the sand particles inside of the agglomerate. There was no agglomeration observed with other biomass fuels in the BFBC. The agglomeration observed with wheat straw pellets combusted at 750 °C could also be due to the poor fluidization, low density and higher porosity as compared with other types of biomass fuels used during combustion. To assess the fuel's chemical nature and the reasons behind these agglomerates, further investigations were performed.

3.4. Analysis of bed material

The results of bed material analysis for all types of tested biomass fuels are presented in Fig. 5(a) and (b). It could be noticed that the bed materials resulting from the combustion of peanut shells and wheat straw contained the highest potassium (K) contents of about 13% and 11%, respectively as compared with other bed materials. Moreover, the industrial wood bed material contained the highest aluminium (Al) content of ca. 10%. All bed materials also contained a sufficient percentage of calcium (Ca) except domestic wood pellets. In the present study, the bed material was a sink of the sand and the ash from biomass with its elements. Usually, less volatile elements such as Al, Si, Mg, P and Ca are present in the bed material but some of the other elements with more volatile characteristics like Na and K as found in the study of Gogolev et al. [28] are less often to be retained in the bed material. From the previous observations was found that wheat straw bed material was affected by agglomeration and that it is the biomass fuel left with the second highest K content in the bed material. Moreover, the higher the element retained in the bed, the fewer emissions are associated with that element in the stack. It is also apparent from Fig. 5(a) that K was the element mostly retained in the bed material compared with all other elements. When sand (quartz) was used as the bed material in FBC systems, the ash formed during combustion could act as a glue or binding medium in the formation of agglomerates as observed in the study of Sevonius et al. [29].

Hence, it is significant to determine how the components from ash are transported to the surface of the sand particles. During combustion, the temperature inside the burning particle of char could be significantly higher than that of the bed material. The high temperature could cause the inorganic matter inside the particles to come out to the surfaces. When the bed particles hit the burning particles, they could stick together forming the agglomerates. The burning particles may be molten

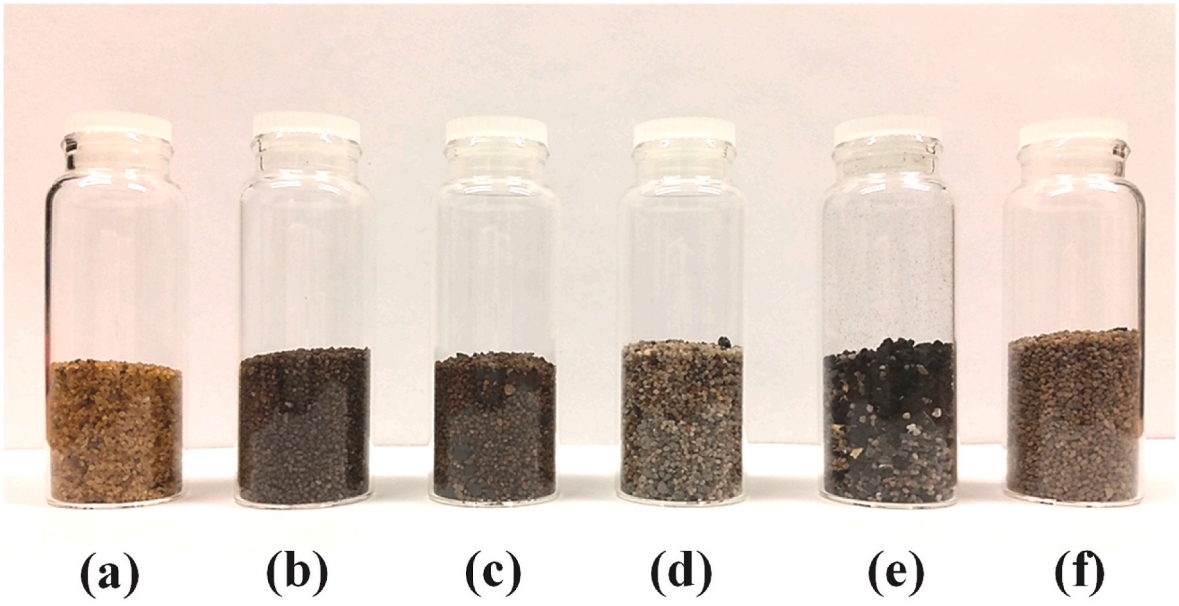

Fig. 4. Bed material samples collected from different biomass fuels; (a) fresh sand, (b) domestic wood, (c) industrial wood, (d) miscanthus, (e) wheat straw and (f) peanut shell.

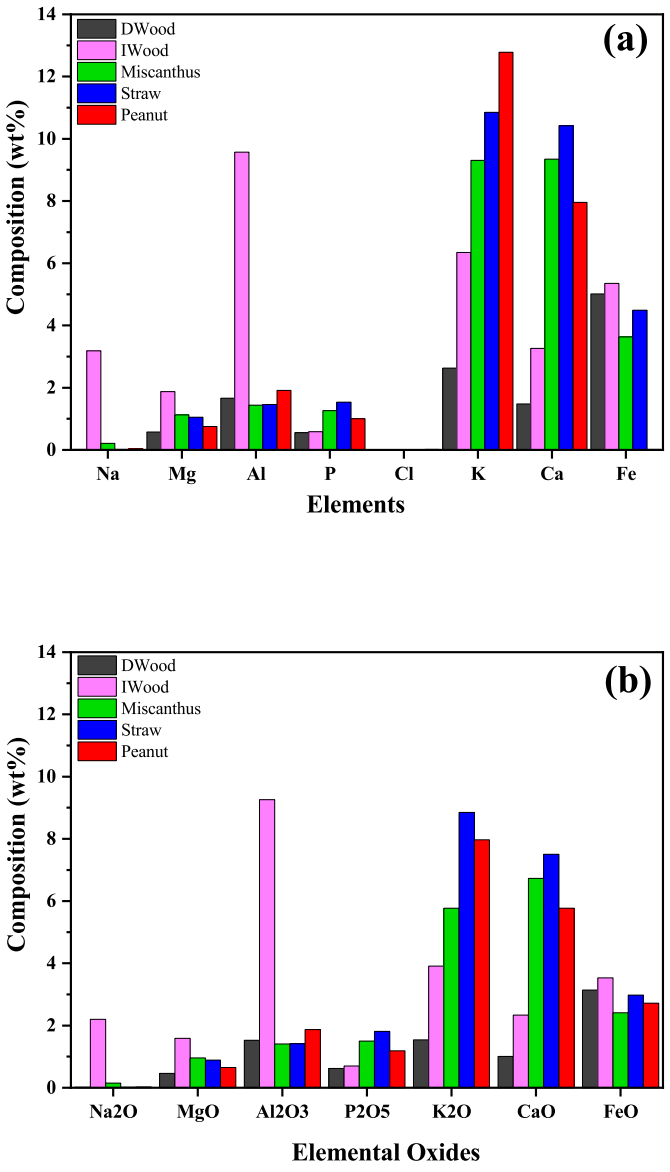

Fig. 5. XRF analysis of bed material obtained from different biomass fuels under air combustion; (a) elemental composition and (b) elemental oxides. Results are given as C and O free basis.

at bed temperatures as low as 750 °C, making the particles a binding medium and catching the sand particles upon collisions. At temperatures as high as 900 °C or above, the burning particles could be completely molten and come in the form of a viscous liquid. When the sand particles collide with these burning particles the liquid could be coated on the surface of the solid bed particles. The condensation of gas evaporated from the burning particles at the surface of bed particles at high temperatures is another possible way of coating formation. Kuba et al. [30] reported about agglomeration phenomena in fluidised bed combustion of wheat straw and other materials and found that K-rich crystals on the surfaces of the bed material were responsible for the coating formation route. The studied biomass fuels are also enriched with Ca, but Ca is unlikely to be considered as the main player in the formation of agglomeration due to high melting points of its compounds [22]. Moreover, some literature reports that K and Na are the two principal elements backing agglomeration during FBs combustion [31]; additionally, Ca decreases agglomeration potential rather than taking a part in this process [32].

Various mechanisms are anticipated for the interactions between ash and bed material particles. Öhman et al. [33] proposed three stages of the agglomeration mechanism based on their experimental studies. First of all, ash is deposited on the bed material surface through a combination of the small particles' attachment on the bed particle surface followed by the gaseous alkali condensation and chemical reaction of the bed material surface with these alkali species. Secondly, as the constant deposition on the bed particles continues, the internal coating layer is perhaps homogenised and reinforced by sintering and finally the agglomeration of bed particles, is controlled by inter-particle adhesive forces. As temperatures increase during FB combustion, the fraction of ash melting increases and the viscosity of this melted substance decreases. As a result of the combination of these factors, the stickiness strength of the bed sand particle coated with ash increases. This finally accelerates the agglomeration process.

The wheat straw behaviour was quite different during combustion in FBs. The wheat straw ash started melting even at a low temperature of 750 °C and only a small fraction of ash was left to evaporate at higher temperatures. It is already mentioned that the temperatures during this study were between 750 and 850 °C. Most probably during these temperatures the wheat straw ash had already started melting, hence these observations correlate with those presented by Morris et al. [34]. After this, the potassium starts accumulating in the bed during combustion that increases with time. Therefore, small amount of potassium was released to the gas phase during wheat straw combustion in BFBC, which is also indicated in Fig. 5(a) and (b) showing high K content. The XRD spectrum of wheat straw cyclone ash is shown in Fig. 6 the K element present in the wheat straw pellets was converted into Sylvite (KCl) at about 52%. Moreover, the wheat straw bed material's XRD analysis also indicated the presence of Sylvite (KCl). The results indicate that the coating on the surface of the bed particle may be too thin to be exactly detected by this method. The peanut shell was found as a biomass fuel with the highest potassium content but it did not show any type of agglomeration during combustion. Hence, as proposed in the study of Atallah et al. [35] the possible cause for no agglomerates forming is probably due to the different volatilisation temperatures of potassium in various biomasses.

3.5. Cyclone ash analysis

The biomass ash characteristics are usually different from other fuels such as coal. The composition is dependent on the type of biomass plant and harvesting conditions. The main elemental ash compositions of all tested biomass fuels are presented in Fig. 7(a). Biomass ash is normally dominated by calcium (Ca), silicon (Si), potassium (K) and a small amount of aluminium (Al) [36]. Si is primarily present in the form of hydrated silica grains [37], while K is spread in the form of ionic and organometallics [38]. The studied biomasses have similar ash elemental compositions as reported by others in the literature. The peanut shell and wheat straw had the highest K content, whereas the industrial wood ash contained the highest Ca content as compared with other biomasses. The K is most likely to be volatilised with other organic species during the combustion process. If chlorine (Cl) is present in the fuel then it may be released in the form of KCl, while in the absence of chlorine, carbonates, oxides, hydroxides or sulphates could be formed [39].

It is also clear from the XRD spectrum results of wheat straw that most of the K is converted into Sylvite (KCl) that contributes to the formation of agglomerates during combustion. The main elemental oxides present in the ash of studied biomass fuels are presented in Fig. 7(b). The results showed that wheat straw had the highest K_2O content followed by peanut shell and miscanthus, respectively. It has been reported that ash with less alkali element, higher Al and less Ca is expected to reduce deposition and corrosion problems during the combustion of woody biomasses in FBs [40]. Niu et al. [13] studied ash-related issues during the combustion of biomass and they reported that during ash formation the alkali and alkaline earth metal ions present in biomass were primarily associated with carbonate, sulphate and chloride ions.

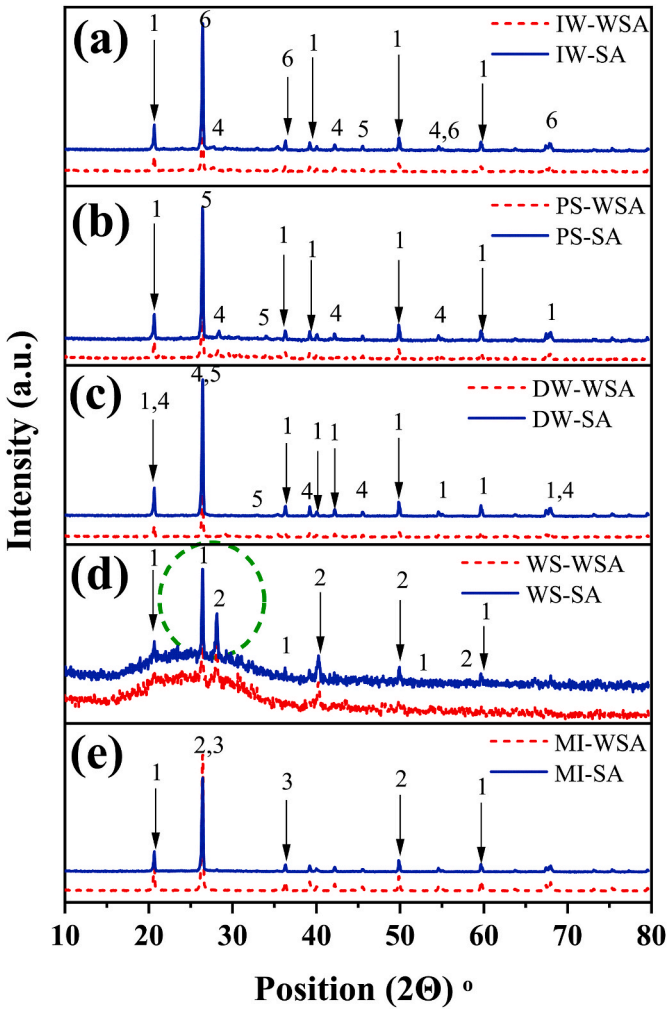

Fig. 6. XRD spectrum of different biomass (IW-industrial wood; PS-peanut shell; DW-domestic wood; WS- wheat straw; MI-miscanthus) under; (a) staging air (SA) and without staging air (WSA) conditions. (1. Quartz, 2. Sylvite, 3. Sodium phosphate hydrogen peroxide, 4. Coesite, 5. Hematite and 6. Albite).

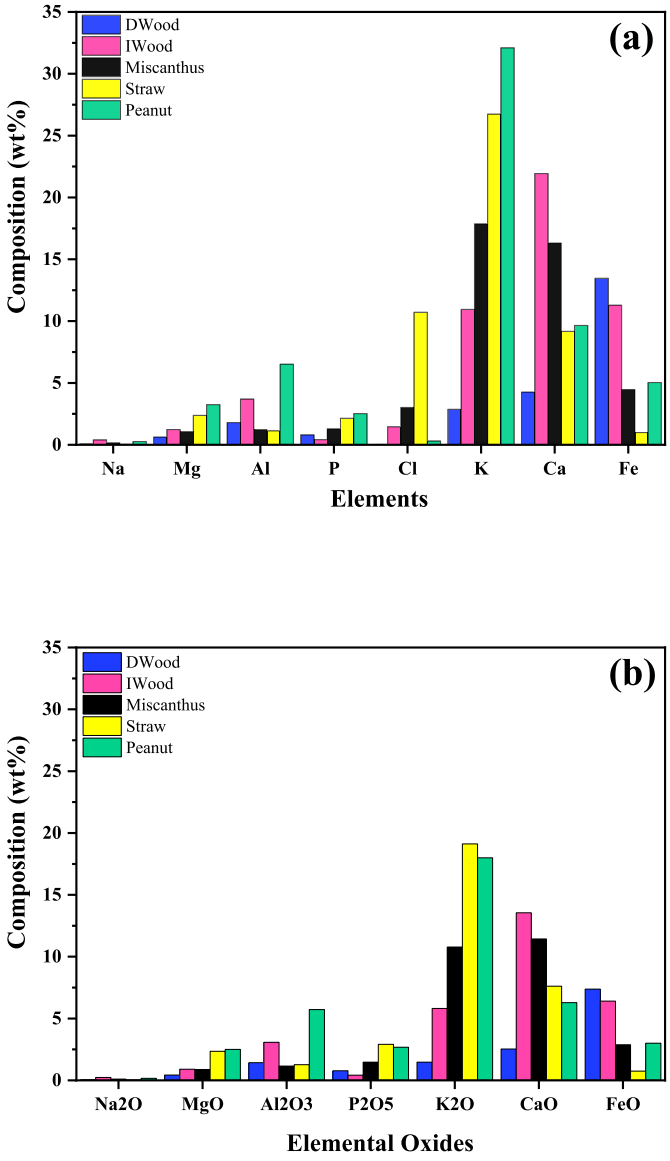

Fig. 7. The XRF results for the cyclone ash obtained from different biomass fuels under air combustion; (a) elemental composition and (b) elemental oxides. (Presented results are Si free basis).

Xiao et al. [41] found that ashing temperatures within the range of 700–900 °C have not significantly affected the elemental composition of the ash. This further indicates that the K compounds may not be released to the gas phase during FB combustion but tend to remain in the ash by recapturing the vapours by some other mineral compounds present in the ash. It is also evident from Fig. 7(a) that most of the K contained in the wheat straw biomass was converted to K_2O (about 19%). This indicates that K_2O-rich ash helps in glueing the particles together and finally creating agglomerates. It has also been observed by other researchers that the presence of K is seen to be an acute contributor to the formation of agglomeration [31].

Thus biomass fuels containing high K_2O are also more likely to cause agglomeration during combustion [42]. Several researchers have reported agglomeration and de-fluidization occurrence in fluidised bed biomass combustion and gasification. Nisamaneenate et al. [43] studied rice straw gasification in a fluidised bed using a bed material of silica sand. They found that the effect of temperature on defluidization time has decreased significantly, which indicated a more pronounced influence of reaction temperature on bed agglomeration. Furthermore, their findings disclosed that the main contributor to the agglomeration phenomenon was the high content of K in the wheat straw ash. Hupa et al. [44] reported defluidisation problems due to agglomeration in continuously fired BFBC that finally led to the plant shutdown. Considering the results from the mentioned study, the possible reason was the presence of alkali silicates in biomass which melt at low temperatures during combustion.

3.6. Surface morphology and spot analysis

A perfect way to identify the constituents that encourage agglomeration is to analyse the coated surface of the particles. For this reason, all types of bed materials along with agglomerates sampled during experiments were physically observed and then examined by SEM-EDX analysis. The agglomerates collected from the bed's sand were very hard and were not breakable by fingers. The agglomerates were in a different size (~4 mm) from the fresh sand and some of them were a few sand grains glued together and in black colour. Numerous SEM-EDX analyses were performed on different types of studied bed materials and agglomerates. Some of the most illustrative and explanatory SEM results are discussed in this section. The typical images captured for different bed materials from SEM are shown in Fig. 8. Domestic wood and miscanthus pellets bed materials showed some broken and damaged sand particles.

On the other hand, industrial wood bed material was seen to contain

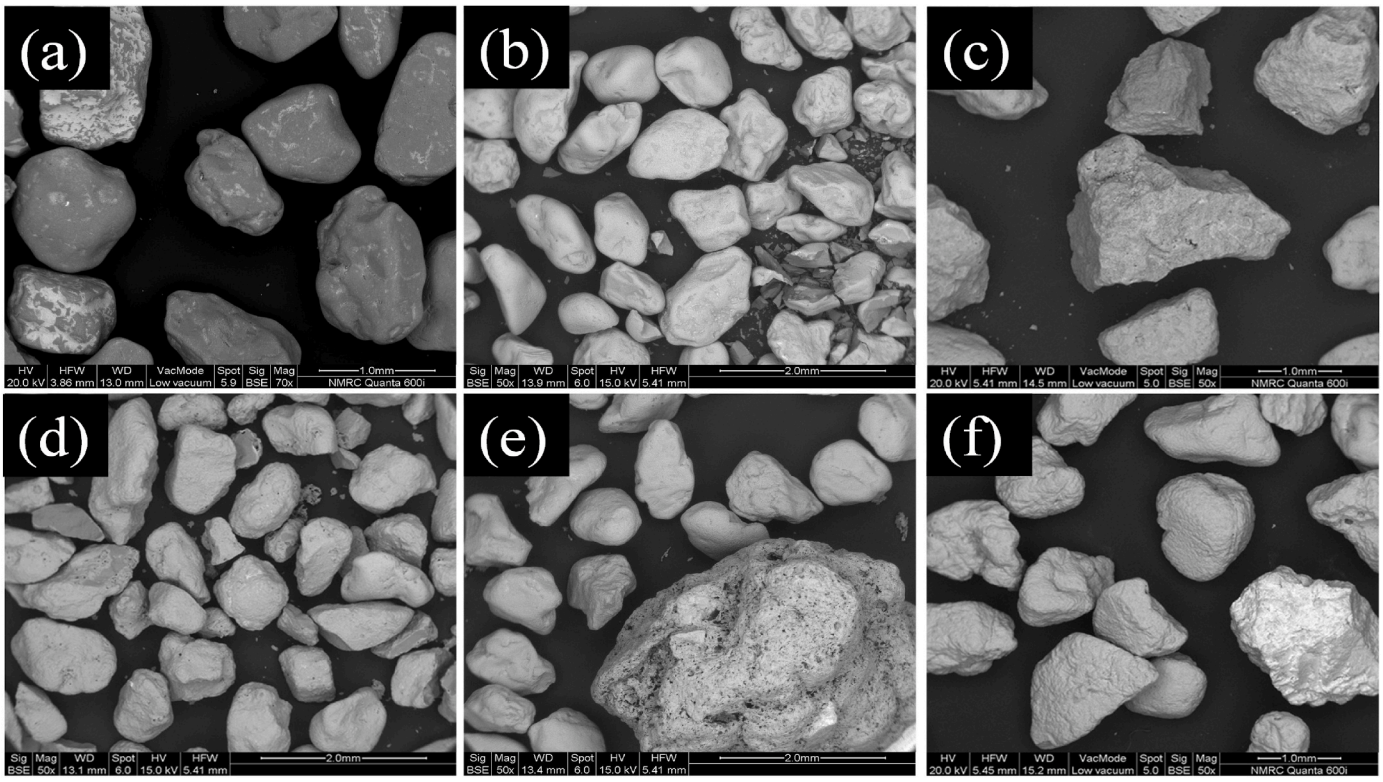

Fig. 8. SEM micrographs from different bed materials; (a) fresh sand, (b) domestic wood, (c) industrial wood, (d) miscanthus, (e) wheat straw and (f) peanut shell.

some sharp edge sand particles. This change in the shape of the bed particles could be associated with different fluid dynamic behaviours during biomass combustion at different temperatures in BFBC. The peanut bed particles looked shiny with polished surfaces. In wheat straw agglomerates the ash flakes were linked with bed particles and some particles were attached by necks. Most of the grain surfaces were covered with ash but some surfaces were smooth as well. It was also noticeable from SEM images that bounded and/or coated particles have an appearance which is glossy and gives an implication of a molten viscous liquid presence during combustion in BFBC. Similar results are reported in the study of Nascimento et al. [10]. The surface morphology analysis (SEM) of typical agglomerates from wheat straw bed material is shown in Fig. 9. The ash and agglomerate appearances suggest that the wheat straw ash has been melted and the holes on the SEM image are evident suggesting that evaporation from inside has occurred. The bed particles were either glued with ash or necked together by the molten substance on their surfaces. Morris et al. [34] reported that wheat straw pellet due to a "ready-made" agglomerate-like structure releases molten ash on the pellet structure to which bed material was sticking.

The SEM micrograms also showed that the layer of coating on the surface of the bed particle was not uniform but with variable thicknesses. Even though there was no coating layer on some particles or partially coated surfaces as could be seen in Fig. 8. These non-uniform coating layers that do occur are enough for the formation of agglomerates and therefore a hindrance to the performance of the BFBC. Van Eyk et al. [45] reported a similar type of mechanism while controlling agglomeration in a circulating fluidised bed during the combustion of low-rank coal. They found that the surface tension, thickness and viscosity of the sticky layers were adequate for the formation of agglomerates. This is believed that the agglomerates formed during this study could grow to substantial sizes with increasing quantity in a longer period of operation.

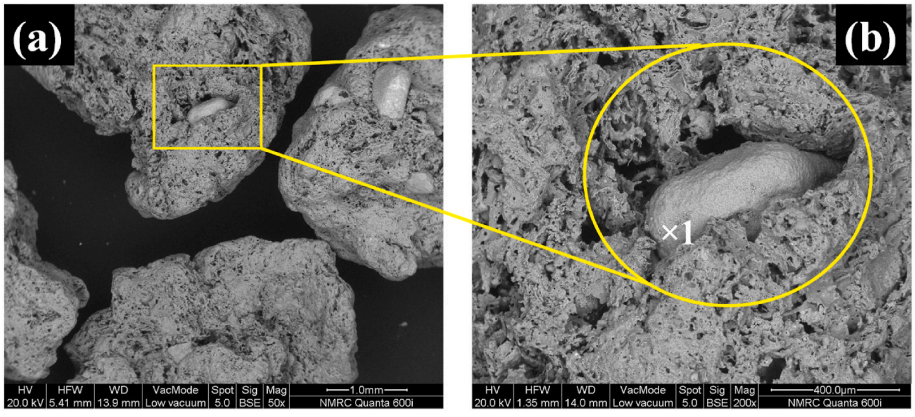

Fig. 9. SEM micrograph images showing internal structure of agglomerated bed material at different magnifications; (a) agglomerated bed materials particles and (b) typical agglomerated particle magnified showing the spot analysis point.

For a better understanding and to know the exact chemical composition of the agglomerate formed, an elemental EDX spot analysis with mapping was performed, the white cross at point 1 marked in Fig. 9 identifies the precise location of the spot where analysis was performed. The analysis found the major elements Si, K and Ca and traces of Al. These typical elements are also present in the form of SiO_2, K_2O and CaO. The K was found to be the second most abundant element after Ca (Ca-19.06%, K-14.24%). The most abundant elemental oxides are SiO_2 (42.04%), CaO (26.66%) and K_2O (17.15%). The SEM and elemental EDX spot analysis findings confirm that not only wheat straw ash combine the bed particles but the rich coating of K on the particle smooth surfaces also contributes towards stickiness in agglomerates. This layer of coating could be present in the liquid phase during combustion that could be the possible reason for agglomeration.

3.7. Control of agglomeration

Agglomeration is considered a serious technical issue during FBs combustion that could result in defluidisation but not under all conditions. Defluidization could occur once the rate of particle agglomeration is greater than the particle separation rate [46]. As previously concluded from the results of this study, the agglomeration was caused by the development of a low melting point eutectic as the result of the reaction between vaporised alkali potassium (K) and bed material, silicon (Si). Therefore, some suggestions to avoid the formation of agglomeration during BFB combustion are as; (1) use of greater particle diameter bed material because bigger particles have less overall surface area, (2) use of alternative bed material that does not cause agglomeration at specific operating temperatures and (3) use of bed additives that could bind volatilised alkali before it reacts with bed particles and finally controlled operating temperatures in the utilized combustor.

4. Conclusion

The experimental results of bed material and ash generated in a pilot scale BFBC burning five different types of biomass fuels were presented and discussed. All bed materials and ash from cyclones from the combustion of various biomasses were regularly sampled and then analysed by SEM-EDX, XRD and XRF analysis. The experimental results showed that the elemental ash composition of the biomass and operating temperature are important parameters affecting agglomeration. All the experiments were conducted under similar combustion conditions with varying levels of stoichiometry. Combustion efficiency of all investigated biomasses ranged from 95.5 to 99.5% and highest efficiency was obtained for miscanthus under SA1 and SA2 conditions, followed by wood pellets with 99% under SA2 using 45% excess air. There was no agglomeration detected except for the combustion of wheat straw and this indicates that combustion stoichiometry has no or minor effect on the agglomeration. The SEM-EDX analysis showed there are substantial differences in the structures and compositions of the agglomerates from wheat straw and other tested biomasses. The highest potassium (K) content of about 13% and 11% were found for peanut shells and wheat straw. Hence, agglomeration formed during combustion in wheat straw ash was largely caused due to the great amount of K. The potassium in wheat straw involves a conversion from organic and inorganic components to various amorphous salts. Most of these compounds tend to stay in the bed below 900 °C that is the top-end operating temperature in FBs combustion. Considering experimental results and different agglomeration mechanisms, the melting of these compounds is defined as the coating layer on the bed particles that eventually form the agglomerates. There are some alternative methods that could be utilized to avoid agglomeration during BFBC such as using alternative bed material, reducing combustion temperatures or using bed additives.

CRediT authorship contribution statement

Farooq Sher: Conceptualization, Methodology, Data curation, Investigation, Formal analysis, Writing – original draft, Funding acquisition, Writing – review & editing. **Narcisa Smječanin:** Visualization, Software, Project administration, Writing – original draft. **Muhammad Kashif Khan, Imran Shabbir and Salman Ali:** Resources, Validation, Writing – review & editing. **Mohammad Rafe Hatshan:** Funding acquisition, Writing – review & editing. **Irfan Ul Hai:** Investigation, Project administration, Writing – review & editing.

Declaration of competing interest

The authors declare that they have no known competing financial interests or personal relationships that could have appeared to influence the work reported in this paper.

Acknowledgement

The authors are grateful for the financial support from the International Society of Engineering Science and Technology (ISEST), UK. The authors are also grateful to the Researchers Supporting Project number (RSP2024R222), King Saud University, Riyadh, Saudi Arabia, for the financial support.

Abbreviations

SEM	Scanning electron microscope
EDX	Energy dispersive X-ray
XRD	X-ray diffraction
XRF	X-ray fluorescence
WAS	Without staging air
SA	Staging air
BFB	Bubbling fluidised bed
BFBC	Bubbling fluidised bed combustor
FB	Fluidised bed
BSE	Backscattered electron

References

[1] A. Shrivastava, R.K. Sharma, Lignocellulosic biomass based microbial fuel cells: performance and applications, J. Clean. Prod. 361 (2022) 132269.
[2] M. Antar, D. Lyu, M. Nazari, A. Shah, X. Zhou, D.L. Smith, Biomass for a sustainable bioeconomy: an overview of world biomass production and utilization, Renew. Sustain. Energy Rev. 139 (2021) 110691.
[3] R.K. Srivastava, N.P. Shetti, K.R. Reddy, E.E. Kwon, M.N. Nadagouda, T. M. Aminabhavi, Biomass utilization and production of biofuels from carbon neutral materials, Environ. Pollut. 276 (2021) 116731.
[4] J. Arun, T. Sasipraba, K. Gopinath, P. Priyadharsini, S. Nachiappan, N. Nirmala, S. Dawn, N.T.L. Chi, A. Pugazhendhi, Influence of biomass and nanoadditives in dark fermentation for enriched bio-hydrogen production: a detailed mechanistic review on pathway and commercialization challenges, Fuel 327 (2022) 125112.
[5] Y.H. Bello, M.A. Ahmed, S. Ookawara, A.E. Elwardany, Numerical and experimental investigation on air distributor design of fluidized bed reactor of sawdust pyrolysis, Energy 239 (2022) 122179.
[6] Z. Miao, E. Jiang, Z. Hu, Review of agglomeration in biomass chemical looping technology, Fuel 309 (2022) 122199.
[7] H. Namkung, Y.-J. Lee, J.-H. Park, G.-S. Song, J.W. Choi, J.-G. Kim, S.-J. Park, J. C. Park, H.-T. Kim, Y.-C. Choi, Influence of herbaceous biomass ash pre-treated by alkali metal leaching on the agglomeration/sintering and corrosion behaviors, Energy 187 (2019) 115950.
[8] K. Kwong, E. Marek, Combustion of biomass in fluidized beds: a review of key phenomena and future perspectives, Energy Fuels 35 (20) (2021) 16303–16334.
[9] C. Maschowski, P. Kruspan, P. Garra, A.T. Arif, G. Trouvé, R. Gieré, Physicochemical and mineralogical characterization of biomass ash from different power plants in the Upper Rhine Region, Fuel 258 (2019) 116020.
[10] F.R.M. Nascimento, A.M. González, E.E.S. Lora, A. Ratner, J.C.E. Palacio, R. Reinaldo, Bench-scale bubbling fluidized bed systems around the world-Bed agglomeration and collapse: a comprehensive review, Int. J. Hydrogen Energy 46 (36) (2021) 18740–18766.
[11] S. Zhang, S. Sun, N. Gao, C. Quan, C. Wu, Effect of auto thermal biomass gasification on the sintering of simulated ashes, Applications in Energy and Combustion Science 9 (2022) 100054.

[12] E. Garcia, H. Liu, Ilmenite as alternative bed material for the combustion of coal and biomass blends in a fluidised bed combustor to improve combustion performance and reduce agglomeration tendency, Energy 239 (2022) 121913.
[13] Y. Niu, H. Tan, Ash-related issues during biomass combustion: alkali-induced slagging, silicate melt-induced slagging (ash fusion), agglomeration, corrosion, ash utilization, and related countermeasures, Prog. Energy Combust. Sci. 52 (2016) 1–61.
[14] M.A.P. Hetian Chi, Chenggong Sun, Hao Liu, An investigation of lime addition to fuel as a countermeasure to bed agglomeration for the combustion of non-woody biomass fuels in a 20kW$_{th}$ bubbling fluidised bed combustor, Fuel 240 (2019) 349–361.
[15] X. Yao, H. Zhou, K. Xu, Q. Xu, L. Li, Evaluation of the fusion and agglomeration properties of ashes from combustion of biomass, coal and their mixtures and the effects of K2CO3 additives, Fuel 255 (2019) 115829.
[16] K. Wagner, G. Häggström, N. Skoglund, J. Priscak, M. Kuba, M. Öhman, H. Hofbauer, Layer formation mechanism of K-feldspar in bubbling fluidized bed combustion of phosphorus-lean and phosphorus-rich residual biomass, Appl. Energy 248 (2019) 545–554.
[17] F. Sher, M.A. Pans, D.T. Afilaka, C. Sun, H.J.E. Liu, Experimental investigation of woody and non-woody biomass combustion in a bubbling fluidised bed combustor focusing on gaseous emissions and temperature profiles, Energy 141 (2017) 2069–2080.
[18] M.F. Llorente, R.E. Cuadrado, Influence of the amount of bed material on the distribution of biomass inorganic elements in a bubbling fluidised bed combustion pilot plant, Fuel 86 (5–6) (2007) 867–876.
[19] H. Chi, M.A. Pans, C. Sun, H. Liu, Effectiveness of bed additives in abating agglomeration during biomass air/oxy combustion in a fluidised bed combustor, Renew. Energy 185 (2022) 945–958.
[20] H. Rietveld, Line profiles of neutron powder-diffraction peaks for structure refinement, Acta Crystallogr. 22 (1) (1967) 151–152.
[21] Z. Pala, E. Shaw, J. Murray, N. Senin, T. Hussain, Suspension high velocity oxy-fuel spraying of TiO2: a quantitative approach to phase composition, J. Eur. Ceram. Soc. 37 (2) (2017) 801–810.
[22] C. Sevonius, P. Yrjas, D. Lindberg, L. Hupa, Agglomeration tendency of a fluidized bed during addition of different phosphate compounds, Fuel 268 (2020) 117300.
[23] S.J. Park, S.H. Son, J.W. Kook, H.W. Ra, S.J. Yoon, T.-Y. Mun, J.H. Moon, S. M. Yoon, J.H. Kim, Y.K. Kim, Gasification operational characteristics of 20-tons-Per-Day rice husk fluidized-bed reactor, Renew. Energy 169 (2021) 788–798.
[24] S.A. El-Sayed, E.H. Noseir, Simulation of combustion of sesame and broad bean stalks in the freeboard zone inside a pilot-scale bubbling fluidized bed combustor using CFD modeling, Appl. Therm. Eng. 158 (2019) 113767.
[25] V. Del Duca, P. Brachi, R. Chirone, R. Chirone, A. Coppola, M. Miccio, G. Ruoppolo, Binary mixtures of biomass and inert components in fluidized beds: experimental and neural network exploration, Fuel 346 (2023) 128314.
[26] T. Gu, W. Ma, Z. Guo, T. Berning, C. Yin, Stable and clean co-combustion of municipal sewage sludge with solid wastes in a grate boiler: a modeling-based feasibility study, Fuel 328 (2022) 125237.
[27] K. Kwong, A. Harrison, J. Gebers, J. Dennis, E. Marek, Chemical looping combustion of a biomass char in Fe2O3-, CuO-, and SrFeO3− δ-based oxygen carriers, Energy Fuels 36 (17) (2022) 9437–9449.
[28] I. Gogolev, T. Pikkarainen, J. Kauppinen, C. Linderholm, B.-M. Steenari, A. Lyngfelt, Investigation of biomass alkali release in a dual circulating fluidized bed chemical looping combustion system, Fuel 297 (2021) 120743.
[29] C. Sevonius, P. Yrjas, D. Lindberg, L. Hupa, Impact of sodium salts on agglomeration in a laboratory fluidized bed, Fuel 245 (2019) 305–315.
[30] M. Kuba, N. Skoglund, M. Öhman, H. Hofbauer, A review on bed material particle layer formation and its positive influence on the performance of thermo-chemical biomass conversion in fluidized beds, Fuel 291 (2021) 120214.
[31] D.Y. Lu, Y. Tan, M.A. Duchesne, D. McCalden, Potassium capture by ilmenite ore as the bed material during fluidized bed conversion, Fuel 335 (2023) 127008.
[32] Z.-M. He, J.-P. Cao, X.-Y. Zhao, Review of biomass agglomeration for fluidized-bed gasification or combustion processes with a focus on the effect of alkali salts, Energy Fuels 36 (16) (2022) 8925–8947.
[33] M. Öhman, A. Nordin, B.-J. Skrifvars, R. Backman, M. Hupa, Bed agglomeration characteristics during fluidized bed combustion of biomass fuels, Energy Fuels 14 (1) (2000) 169–178.
[34] J.D. Morris, S.S. Daood, W. Nimmo, The use of kaolin and dolomite bed additives as an agglomeration mitigation method for wheat straw and miscanthus biomass fuels in a pilot-scale fluidized bed combustor, Renew. Energy 196 (2022) 749–762.
[35] E. Atallah, F. Defoort, A. Pisch, C. Dupont, Thermodynamic equilibrium approach to predict the inorganic interactions of ash from biomass and their mixtures: a critical assessment, Fuel Process. Technol. 235 (2022) 107369.
[36] T. Leffler, M. Eriksson, B. Leckner, F. Lind, F. Winquist, P. Knutsson, Monitoring of bed material in a biomass fluidized bed boiler using an electronic tongue, Fuel 340 (2023) 127598.
[37] F. Schlupp, J. Page, C. Djelal, L. Libessart, Influence of recycled sand from biomass combustion on the mechanical, hydration and porous properties of mortar mixtures, Construct. Build. Mater. 404 (2023) 133193.
[38] X. Wang, Y. Zhao, J. Deng, Y. Zhou, S. Yuan, Study on the influence mechanism of mineral components in biochar on the adsorption of Cr (VI), Fuel 340 (2023) 127631.
[39] A. Szydełko, W. Ferens, W. Rybak, The effect of mineral additives on the process of chlorine bonding during combustion and co-combustion of Solid Recovered Fuels, Waste Manag. 102 (2020) 624–634.
[40] A. Awasthi, T. Bhaskar, Combustion of lignocellulosic biomass, in: Biofuels: Alternative Feedstocks and Conversion Processes for the Production of Liquid and Gaseous Biofuels, Elsevier, 2019, pp. 267–284.
[41] W. Xiao, S. Wang, B. Wei, J. Wang, L. Chen, K. Liu, T. Wang, Effect of temperature and pressure on the transformation characteristics of inorganic elements in cotton straw ash, Fuel 340 (2023) 127443.
[42] W. Yang, Y. Zhu, Y. Li, W. Cheng, W. Zhang, H. Yang, Z. Tan, H. Chen, Mitigation of particulate matter emissions from co-combustion of rice husk with cotton stalk or cornstalk, Renew. Energy 190 (2022) 893–902.
[43] J. Nisamaneenate, D. Atong, A. Seemen, V. Sricharoenchaikul, Mitigating bed agglomeration in a fluidized bed gasifier operating on rice straw, Energy Rep. 6 (2020) 275–285.
[44] M. Hupa, O. Karlström, E. Vainio, Biomass combustion technology development–It is all about chemical details, Proc. Combust. Inst. 36 (1) (2017) 113–134.
[45] P.J. van Eyk, A. Kosminski, P.J. Mullinger, P.J. Ashman, Control of agglomeration during circulating fluidized bed gasification of a South Australian low-rank coal: pilot scale testing, Energy Fuels 30 (3) (2016) 1771–1782.
[46] S. Orozco, J. Alvarez, G. Lopez, M. Artetxe, J. Bilbao, M. Olazar, Pyrolysis of plastic wastes in a fountain confined conical spouted bed reactor: determination of stable operating conditions, Energy Convers. Manag. 229 (2021) 113768.
[47] S. Channiwala, P. Parikh, A unified correlation for estimating HHV of solid, liquid and gaseous fuels, Fuel 81 (8) (2002) 1051–1063.